Interplay between purging and admixture shapes genetic load in an invasive guppy population

Katarzyna Burda[1]†, Mary J Janecka[2], Ryan S. Mohammed[3,4], David R. Clark[5], Rachael Kramp[5], Jessica F. Stephenson[6], Jacek Radwan[1], Mateusz Konczal[1*]

[1] Evolutionary Biology Group, Faculty of Biology, Adam Mickiewicz University; 60-614 Poznań, Poland

[2] Carnegie Museum of Natural History, Powdermill Nature Reserve, Rector, Pennsylvania, USA

[3] College of Science and Mathematics, Auburn University, Auburn, Alabama, USA

[4] Department of Life Sciences, Faculty of Science and Technology, The University of the West Indies, Trinidad and Tobago.

[5] Department of Biological Sciences, University of Pittsburgh, Pittsburgh, Pennsylvania, USA

[6] Department of Zoology, Stockholm University, Stockholm 106 91, Sweden

† Present address: Department of Genetics and Microbiology, Maria Curie-Skłodowska University, 20-033 Lublin, Poland

* corresponding author: mateusz.konczal@amu.edu.pl

Running title: Genetic load is shaped by purging and admixture

ABSTRACT

Demographic history can shape the genetic load of populations by influencing the efficacy of selection, levels of heterozygosity, and the incorporation of new variants via gene flow. Understanding these dynamics is crucial for identifying threats to population viability and predicting evolutionary trajectories of invasive populations translocated by humans into non-native environments. We investigate these processes in Trinidadian guppies (*Poecilia reticulata*) by estimating genetic loads across multiple populations, with a particular focus on a single expanding population in which translocated individuals have rapidly spread and replaced native individuals. Overall, we observe the expected negative relationship between neutral genetic diversity and relative genetic load. In the translocated population, patterns differ between strongly and weakly deleterious mutations. Strongly deleterious alleles are purged at the isolated translocation site but tend to accumulate along the expansion front. In contrast, the genetic load estimated based on weakly deleterious variants declines along the expansion gradient. These differing patterns can be explained by admixture with native populations (which carried fewer weakly deleterious mutations) reducing the overall genetic load of the population at the expansion front. However, admixture has also increased genetic diversity and introduced new strongly deleterious alleles, thereby reversing the purging effect. Together, our findings illustrate the complex interactions determining genetic load in subdivided populations, offering important insights into the evolutionary aspects of biological invasions.

INTRODUCTION

Genetic load refers to the decrease in fitness caused by deleterious variants in a genome (Crow 1989; Bertorelle et al. 2022). Most of the deleterious mutations have slight effects in heterozygous carriers and remain rare in large panmictic populations (Eyre-Walker and Keightley 2007). Such deleterious variants present in heterozygous genotypes are often referred to as “heterozygous genetic load” (Bertorelle et al. 2022). Under some demographic scenarios, deleterious variants can increase in frequency and become exposed in homozygotes as a “homozygous genetic load”, which may threaten population survival (Mathur and DeWoody 2021). In such a situation, deleterious alleles may either become common, or even fixed, in a population decreasing its mean fitness, or they may be eliminated from the population by “purging” (Dussex et al. 2023; Robinson et al. 2023).

Demographic changes, such as a population reduction, are expected to affect genetic variation and the genetic load of a population through increased genetic drift (Wright 1932) and inbreeding (Wright 1922). Genetic drift increases the variance around the mean frequency of deleterious mutations, allowing some deleterious alleles to drift to high frequencies (de Pedro et al. 2021; Zeitler et al. 2023; Stewart et al. 2017). Thus, in small populations in which selection fails to remove deleterious mutations of weak effects, these variants accumulate over time (Kimura and Ohta 1969) and may eventually fix (Kimura et al. 1963). This accumulation reduces fitness, which may further reduce population size, potentially resulting in a vicious circle of "mutational meltdown" (Lynch et al. 1995). Under this scenario, such "genetic erosion" in small, isolated populations of endangered species should relate to their estimated neutral genetic variation, reflecting "effective population size". In other words, genome-wide genetic variation underlies fitness and thus provide crucial information for conservation (Kardos et al. 2021; DeWoody et al. 2021; Willi et al. 2022). Consistent with these theoretical predictions, a negative relationship between neutral nucleotide diversity and homozygous load was indeed found, for example in an endangered rattlesnake (Mathur et al. 2023a) or Montezuma quail (Mathur et al. 2023b).

However, the relationship between genetic load and neutral diversity depends on the timescale of evolutionary processes that generate these correlations (Mathur et al. 2023a, 2023b) and may be changed by recent demographic events. For instance, a recent transient population size reduction might increase a population's mean fitness through several processes. First, alleles at low frequencies, such as strongly deleterious mutations, are likely to be lost by drift. Second, reduced population size increases the probability that alleles carried by mating partners are identical by descent, leading to increased homozygosity in a population (Wright 1922) thus changing masked load into realized load. Highly deleterious variants at low frequencies in the pre-bottleneck population thus become exposed to natural selection (Charlesworth and Willis 2009). If selection can overcome genetic drift, it may purge large effect deleterious variants, ultimately decreasing both heterozygous and total genetic load (Glémin 2003; Crnokrak and Barrett 2002; Keller and Waller 2002; Barrett and Charlesworth 1991). New genomic data suggest that purging occurs more often than previously thought (Dussex et al. 2023), however, its effectiveness differs between species (Lan et al. 2025) and its consequences for population viability and extinction risk remain unclear (Kardos et al. 2025). Consequently, Teixeira and Huber (2021) argued against the importance of neutral genetic diversity for the conservation of wild populations, and instead

advocated for a better understanding of the properties of non-neutral genetic diversity. Quantitative assessment of functional variation is, however, difficult, and despite wide discussion and studies in multiple systems, there is still no general understanding of how useful such information is for wild populations conservation (Kardos et al. 2023; van Oosterhout et al. 2026; Ralls et al. 2020; Kardos et al. 2021; Robinson et al. 2019; Kyriazis et al. 2021; Kardos et al. 2025).

Such investigations might also be important in the context of biological invasions (Estoup et al. 2016). Even though invasions and endangered species reflect opposite ends of a spectrum of ecological success, they experience similar challenges (Colautti et al. 2017). Both natural and artificial translocations that give rise to invasions usually introduce small numbers of often related individuals, and thus the initial stages of invasion involve small effective population sizes. Maintaining invasive potential despite expected loss of genetic diversity and increased genetic load was termed the "genetic paradox" of invasions (Estoup et al. 2016; Kołodziejczyk et al. 2025). It has been suggested that purging may explain this paradox and contribute to the invasive potential of translocated populations (Estoup et al. 2016). Purging in invasive species has, however, been documented in only a few cases (Facon et al. 2011; Lombaert et al. 2025; Zayed et al. 2007), making generalization difficult. Following an initial bottleneck, invasive species often experience rapid range expansion. Such expansions can involve multiple subsequent bottlenecks, increasing the effects of purging and genetic drift especially at the expansion front (Peischl et al. 2015). This process might then lead to further accumulation of weakly deleterious variants and purging of strongly deleterious ones (Rougemont et al. 2023).

However, following the initial bottleneck, successful invasions are often associated with admixture between divergent genotypes (when translocations occur multiple times) or with hybridization between translocated and native populations (Barker et al. 2019; Kołodziejczyk et al. 2025; Colautti et al. 2017). Potential benefits of such admixture include increased genetic variation and incorporation of alleles associated with local adaption into the genetic pool of invasive species, enabling adaptation to novel habitats (Wagner et al. 2017; Kołodziejczyk et al. 2025). Interestingly, genome-wide genetic diversity was not significantly reduced in many invasive populations, likely due to recent admixture or hybridization (Kołodziejczyk et al. 2025). However, little is known about the effect of these admixture events on the dynamics of genetic load. On one hand, admixture might be expected to mask the homozygous genetic load of an expanding population, not only for deleterious mutations that increased in frequency during past bottlenecks, but also for variants already fixed in

a population. On the other hand, it has the potential to introduce new variants into a population, some of them being deleterious, potentially increasing the total genetic load of an invasive population. It has been suggested for example, that introgression of Neanderthal ancestry into anatomically modern human genomes, during the expansion out of Africa, reduced fitness by at least 0.5%, due to increased genetic load derived from Neanderthal genomes (Harris and Nielsen 2016). However, whether such scenarios can affect invasion potential has rarely been studied.

Here, we examine the fate of genetic load during the invasion of Trinidadian guppies (*Poecilia reticulata*) into a diverged, allopatric population, during which translocated individuals rapidly spread and replaced native individuals. Guppies occur naturally in the fresh waters of Trinidad, Tobago and South America, but have been translocated and successfully invaded multiple sites across the globe (Deacon et al. 2011). Natural Trinidadian populations have been intensively studied by generations of ecologists and evolutionary biologists (Magurran 2005) and some of these studies included translocation experiments (Fitzpatrick et al. 2016; Fraser et al. 2015). One such translocation occurred in the Turure River in 1957 (Endler 1980; Reznick and Bryga 1987; Shaw et al. 1992). Fish from the lower Guanapo River (Caroni drainage) were moved to a site in the upper Turure River (Oropouche drainage) which previously lacked guppies (Magurran 2005). 200 guppies, approximately half females, were introduced (Shaw et al. 1992; Sievers et al. 2012). Importantly, the source and recipient drainages are inhabited by differentiated guppy populations (Willing et al. 2010), with long separate histories (estimated to have split 0.18-1.2 mya, based on net divergence (Fajen and Breden 1992; Whiting et al. 2021)), and evidence of partial reproductive isolation (Russell and Magurran 2006). The Oropouche fish are more diverged from Caroni than from other fish on other islands (e.g. Tobago), suggesting that they may represent distinct species (Schories et al. 2009), though evidence for barriers to gene flow is weak (Devigili et al. 2018; Magurran 2005). The differentiation documented by these studies reflects both isolation and adaptation to different local environments (Reznick et al. 1990; Bassar et al. 2010; Kemp et al. 2018). However, after translocation, genetically foreign individuals spread rapidly, and largely replaced native individuals in the lower parts of the Turure River. Furthermore, several sources of evidence demonstrated ongoing admixture from resident populations (Becher and Magurran 2000; Willing et al. 2010; Sievers et al. 2012).

We aimed to test whether the spread of Guanapo-derived genomes into the resident populations of the Turure River was associated with changes in genetic load. In particular, we test the hypothesis (H1) that the Guanapo-

128 derived population introduced into the upstream Turure was purged of highly deleterious mutations and now
129 has a low overall genetic load, potentially increasing invasive potential (Sievers et al. 2012). To test this
130 hypothesis, we compared the genetic load of the upstream Turure population with that of the Guanapo source
131 population. Additionally, we explore the accumulation of genetic load along the Turure River, to test the
132 hypothesis (H2) of expansion associated with a series of bottlenecks, allowing the accumulation of weakly
133 deleterious mutations and the purging of strongly deleterious mutations in downriver sites. However, if
134 admixture occurred along with expansion, as earlier work suggests (Sievers et al. 2012; Willing et al. 2010),
135 genetic load might also be affected by this process. We therefore explore differences in both genetic load and
136 admixture along the river. Additionally, to provide a benchmark for interpreting genetic load in our focal
137 populations, we test for associations between neutral diversity and genetic load across multiple populations
138 from other rivers. Guppy populations in Trinidadian rivers range in population size from hundreds to tens of
139 thousands of individuals (Whiting et al. 2021), providing the opportunity to test for such an association.

140

141 **RESULTS**

142 ***Population structure and nucleotide diversity***

143 We analyzed 201 individuals from 15 populations (sampling sites) originating from nine rivers on Trinidad
144 (Aripo, Caura, Guanapo, Lopinot, Santa Cruz, La Seiva, Oropouche, Quare, Turure), and two rivers on Tobago
145 (Dog River and Roxborough; Fig. 1B; Supplemental Table S1). Five analyzed Trinidadian rivers belong to the
146 Caroni drainage and the other four to the Oropouche drainage. Three rivers were sampled in more than one
147 location: Quare (upper and lower), Oropouche (upper and lower), and Turure (upper, middle and lower).
148 Samples were sequenced yielding a mean coverage of 15x (7x - 36x) and were mapped to the reference genome
149 with over 97% reads aligned in all individuals sampled.

150 We performed principal component analysis (PCA) to understand the overall pattern of genetic differentiation
151 between populations. The first PC (explaining 22.2% variation) separated Oropouche (which included the
152 Turure, recipient river) from the Caroni (which included the Guanapo, source river) drainages, whereas the
153 second, explained 13.8% of variation, separated samples from Trinidad from those on Tobago (Fig.1C). Turure

individuals cluster with the Guanapo population. Individuals from the lower Quare River sites have intermediate positions on PC1, and cluster with neither Caroni nor other Oropuche drainage individuals, consistent with other strong signals of admixture in this population (Willing et al. 2010; Fitzpatrick et al. 2016; Whiting et al. 2021).

Admixture analysis identified the optimal K-value as 12, with clear differentiation among the two islands and the Trinidad drainages (Fig. 1A). The upper and lower Oropouche sites are highly similar to each other, whereas the upper and lower Quare sites differ, with greater variation in the lower site. In the upper Turure River, to which Caroni drainage fish were translocated, we found high similarity to the Guanapo source population and no evidence of admixture, in accordance with previous findings (Willing et al. 2010). As expected, increased admixture is detected downstream, probably reflecting crosses between introduced and native populations, although the vast majority of the ancestry is from the introduced population (Fig. 1A).

Interestingly, we observed 5 individuals from the Turure middle site, that cluster separately from the other samples from the same site (Fig. 1C). In the admixture plot they represent pure distinct genetic ancestry, while one other individual from the same population seems to be F1 hybrid, and others seem to be admixed for this ancestry (marked as grey triangles in Figs. 1A and 1C). These individuals come from two different sampling years, making it unlikely that they represent mislabeling or other errors. Most likely, these individuals represent a truly distinct genetic population within this river, possibly due to another recent translocation from an unknown source. These five individuals and the putative F1 hybrid were excluded from the analyses below.

Genome-wide nucleotide diversity estimates for 4-fold degenerated sites range from $2.3 \cdot 10^{-3}$ to $6.5 \cdot 10^{-3}$ per site, with the estimate for the upper Turure site being relatively similar to that for Guanapo source population ($3.22 \cdot 10^{-3}$ vs $2.67 \cdot 10^{-3}$, Fig. 2). Analyses of the lower sites in all rivers, but excluding the post-translocation Turure populations, showed higher diversity in Oropouche (in intercept) than Caroni populations (estimate = -0.0022, se=0.0006, t= -2.899, p= 0.023) and Tobago (estimate = -0.0028, SE=0.0008, t= -3.495, p = 0.010).

To assess whether the translocated population exhibits signals of recent bottlenecks, we estimated Tajima's D values. Negative Tajima's D values indicate an excess of rare variants relative to neutral expectation under drift-mutation equilibrium. This can be caused by recent population growth or by negative selection acting against mutations, whereas a positive Tajima's D indicates an excess of common variants suggesting balancing

181 selection, population structure, or a recent bottleneck that caused loss of rare variants. Our estimates based on
182 4-fold degenerated sites should thus reflect mostly demographic differences. Upstream sites showed
183 significantly higher Tajima's D values than downstream sites, and the upper Turure had higher values than its
184 source Guanapo population (Supplemental Fig. S1). However, the difference between Guanapo and the upper
185 Tururre site was smaller than that of many Oropouche populations, thus the allele frequency spectrum in this
186 population suggests only subtle effects of the translocation event.

187 ***Genetic load and its correlation with neutral diversity***

188 We calculated three measures of genetic load for each re-sequenced individual: *Relative Loss-of-Function Load*
189 (RLL), *Relative Genetic Load* (RGL) and *Relative Missense Load* (RML). The three measures are expected to
190 reflect the effects of different classes of deleterious mutations. As loss-of-function (LoF) mutations are
191 expected to be the most severe, with large expected effects on individual fitness on average, thus we used RLL
192 to reflect the effects of the most deleterious class of mutations. The RGL estimate was based on conservation
193 scores (CS) calculated from the observed number of substitutions in a multi-species alignment, relative to the
194 number of expected substitutions under neutrality (Davydov et al. 2010). This provides information
195 on evolutionary constraints. Mutations with high CS scores, have been used to estimate genetic load in many
196 studies and are already a well-established approach (Bertorelle et al. 2022) that likely captures a wider range
197 of selection coefficients than LoF mutations. Finally, many missense mutations are weakly deleterious, thus
198 the genetic load estimated from these variants (RML) should reflect the least deleterious classes of mutations.

199 To estimate genetic load, the guppy reference genome was first polarized using Illumina data from two
200 outgroup species, *Xiphophorus maculatus* and *Micropoecilia picta* (14x and 23x coverage, respectively). We
201 inferred ancestral states for the sites used in CS analyses; 42,860,381 sites (5.9% of the genome) yielded
202 information about both ancestral allele and CS. We called genotypes for these sites separately within each
203 guppy population using stringent filtering criteria (see Supplemental Tab. S2 for effects of filtering on the
204 number of called genotypes). RGL value was then calculated per individual, as the sum of presumably
205 deleterious mutations (CS>2) weighted by the CS value, relative to the value for all derived variants. RLL and
206 RML were respectively calculated as the ratio of loss-of-function (LoF) and missense derived variant numbers
207 to the number of derived synonymous variants in an individual's genome. All three values (RGL, RLL and

208 RML) were calculated separately for homozygous and heterozygous genotypes. The sum of these two
209 approximates the total genetic load. We used the value of CS>2 as a threshold to balance selectivity and sample
210 size (higher CS values included very small numbers of SNPs; Supplemental Table S3). In total, we analyzed
211 1659383 sites, including 3479 with CS > 2. The coding regions were enriched in polymorphic sites with CS>2,
212 when compared with intergenic regions, and nonsynonymous variants were enriched in such sites when
213 compared with synonymous ones, demonstrating that conservation scores can capture deleterious variation.
214 Populations show considerable variation in the mean number of putatively deleterious variants per individual
215 despite little variation in coverage across populations (Supplemental Table S4).

216 Genetic load differed among geographic regions, with Oropouche populations generally having the lowest
217 load, significantly lower than Tobago in most comparisons (total RGL, homozygous RGL, total RML,
218 homozygous RML and heterozygous RLL, Supplemental Table S5) and lower than Caroni for total RGL
219 (Supplemental Table S5). Consequently, in models predicting genetic load from nucleotide diversity in a
220 population after accounting for regional differences we only found a significant negative association between
221 nucleotide diversity and total RGL (estimate = -2.451, SE=0.798, t= -3.069, P=0.022; Fig. 3), and the region
222 was not significant in any of these analyses. After removing the region, we found that total RGL and total RML
223 were negatively associated with nucleotide diversity, whereas total RLL was not significantly predicted by
224 nucleotide diversity (Supplemental Table S6, Fig. 3). Nucleotide diversity was also found to be negatively
225 associated with homozygous RGL (Supplemental Table S6, Supplemental Fig. S2).

226 For the two rivers with samples suitable for analysis, Oropouche and Quare, our comparisons of upstream
227 versus downstream populations agreed with previous studies (Willing et al. 2010; Qiu et al. 2022), and
228 generally support lower effective sizes and/or bottlenecks experienced during upstream colonization. As
229 expected, guppies from upstream sites tended to have higher load by almost all measures, except for
230 heterozygous RLL (Supplemental Table S7 and Supplemental Fig. S3).

231 ***Genetic load in the translocated and expanding population***

232 To test hypothesis H1, we compared Guanapo (source) and upper Tururе (translocated) populations. The results
233 showed a complex pattern of differences in genetic load (Supplemental Table S8, Fig. 4). The upper Tururе
234 had significantly lower values of total and heterozygous RGL and RML, but higher homozygous RML than

235 the Guanapo. For RLL, however, the upper Tururе had significantly lower load on all three measures than the
236 Guanapo.

237 Focusing on the three Tururе populations (hypothesis H2), we found that upper Tururе had significantly higher
238 RGL and RML compared to downstream populations, except for heterozygous RML and heterozygous RGL,
239 which did not differ significantly from those of lower Tururе guppies (Supplemental Table S9, Fig. 5).
240 Remarkably, the pattern was reversed for RLL: upper Tururе had significantly lower total, heterozygous and
241 homozygous RLL compared to lower Tururе, and also marginally lower homozygous RLL compared to middle
242 Tururе (Supplemental Table S9, Fig. 5).

243

244 **DISCUSSION**

245 The accelerating pace of global change, driven by climate shifts and habitat loss, has led to widespread species
246 migration, range fragmentation, and population isolation (Johnson et al. 2017). These rapid demographic shifts
247 can profoundly influence the dynamics of genetic load, posing challenges for conservation biology. To date,
248 most research in this area has centered on endangered, highly vulnerable, or even extinct taxa (Kuang et al.
249 2020; Von Seth et al. 2021; Kleinman-Ruiz et al. 2022; Ochoa et al. 2022; Xie et al. 2022). The role of genetic
250 load in biological invasions has received less attention (de Pedro et al. 2021; Rougemont et al. 2020; Tayeh et
251 al. 2013). Our study addresses this gap by investigating how genetic load accumulates in invasive, non-
252 threatened species (Deacon et al. 2011; Lindholm et al. 2005; Rosenthal et al. 2021), thereby offering insights
253 into the mechanisms of invasion—particularly when accompanied by admixture with native populations. Our
254 large population-genomic dataset of hundreds of guppy genomes from multiple wild populations shows that
255 genetic loads are strongly affected by historical effective population size (inferred from neutral diversity). We
256 also found that translocated populations appear to have purged strongly deleterious mutations, and that
257 subsequent admixture along the expansion gradient restored this load.

258 ***Genetic load correlates with historical effective population sizes***

259 Population genetics and conservation biology have long focused on how changes in population sizes shape the
260 amount and distribution of deleterious variation (Bertorelle et al. 2022; van Oosterhout et al. 2026; Dussex et

261 al. 2023; Robinson et al. 2023; Kimura et al. 1963; Lande 1998; Lynch et al. 1995). Theoretical and empirical
262 evidence suggest that prolonged reductions in effective population size, or bottlenecks lasting hundreds or
263 thousands of generations, should allow weakly to moderately deleterious alleles to accumulate, although
264 strongly deleterious alleles might also be purged (Xue et al. 2015; Robinson et al. 2018; Dussex et al. 2021;
265 Mathur and DeWoody 2021; Kleinman-Ruiz et al. 2022). Therefore, when measured based on mildly
266 deleterious alleles, genetic load estimates should correlate with long-term Ne (or neutral nucleotide diversity).
267 Testing these predictions using inter-species comparisons has produced mixed results: although some studies
268 reported the expected correlations (Schmidt et al. 2023; Wilder et al. 2023), another reported no correlation
269 (Wooldridge et al. 2024). However, no consistent general framework exists for comparing genetic load across
270 species (Dussex et al. 2023; Teixeira and Huber 2021). Further, endangered species - the typical focus of such
271 work - rarely contain multiple populations with contrasting demographic histories and a broad range of
272 effective population sizes. Intraspecific associations between Ne and genetic load have thus been studied in
273 only a handful of cases (Kleinman-Ruiz et al. 2022; Mathur and DeWoody 2021; Smeds et al. 2024; Mathur
274 et al. 2023a; Grossen et al. 2020). Our intraspecific analyses therefore provide valuable insight, showing that
275 the expected negative relationship between neutral nucleotide diversity and relative genetic load is
276 detectable—particularly when comparing a broad spectrum of mutation types, as estimated by RGL and RML.
277 Additionally, a significant relationship increased our confidence in the methods used to infer genetic load.
278 These methods rely on predicted mutation effects and thus depend on the quality of annotation. Annotation
279 used here is based on an ensemble pipeline and should be free of major issues, however, even in model species
280 loss-of-function mutations tend to be enriched for annotation errors (Karczewski et al. 2020). While more
281 sophisticated approaches for assessing variant impact are available, (Avsec et al. 2025; Cheng et al. 2023;
282 Speak et al. 2023), they require large training datasets and are still rarely applied in conservation genomics.
283 Our results demonstrate that methods based on simpler conservation scores can provide useful tools for wildlife
284 population genomics.

285 ***Purging in translocated populations of invasive potential***

286 Our conclusion that the post-bottleneck Turure upper population experienced purging is based on distinct
287 patterns observed for RLL, the load reflecting the most strongly deleterious mutations, in comparison with
288 load estimates based on wider ranges of mutation effects (RML and RGL). A population bottleneck alone does

not affect expected frequencies of variants, but increases variance in these frequencies and thus increases homozygosity. Consequently, under increased genetic drift alone, homozygous load is predicted to increase while heterozygous load should decline, and total genetic load should remain unchanged assuming intermediate effects of all variants in heterozygotes (Dussex et al. 2023; García-Dorado 2012). We detected the expected changes in heterozygous and homozygous loads when comparing source and translocated populations' RML and RGL values (Fig. 4), though the total values have decreased in the translocated populations, possibly due to selection purging the most deleterious variants in homozygous genotypes. As expected (Glémin 2003; Caballero et al. 2017; Dussex et al. 2023), the bottleneck effect is most pronounced for strongly deleterious mutations: all three classes of RLL (total, heterozygous and homozygous) decreased following translocation. We acknowledge that the comparison of the Guanapo source population and the Tururе translocated populations may be confounded by batch effects, as we used publicly available data from Guanapo. However, we controlled for sequencing depth in our analyses, and the batch effect that could have resulted from other sources was generally weak in the remaining populations. Furthermore, any bias would likely affect all classes of mutations similarly, synonymous ones including; therefore, given that our genetic load estimates are relative to synonymous ones, we do not expect this to substantially affect our overall results or interpretation. Finally, observation of different patterns using different classes of inferred mutations, as discussed above, cannot be reconciled with batch effect.

Effects on loads after bottlenecks similar to those we found have been documented in other species (Grossen et al. 2020; Khan et al. 2021; Quinn et al. 2024; Ochoa and Gibbs 2021; Xue et al. 2015; Stuart et al. 2025). Collectively, these findings provide strong evidence for purging (Dussex et al. 2023), suggesting that, under suitable conditions, highly deleterious mutations can be removed from bottlenecked populations, potentially increasing their invasiveness (Estoup et al. 2016).

The Tururе population, which we infer to be purged of the most strongly deleterious mutations, exhibits marked invasive potential, a possibility first raised when indigenous guppies were observed to be displaced (Becher and Magurran 2000; Shaw et al. 1992). Early genetic studies using allozymes confirmed that the translocated individuals established a viable population, overcame the natural waterfall barrier—likely aided by flooding events—and began spreading into different downstream environments (Shaw et al. 1992). Subsequent analyses of a panel of SNPs showed that fish from the middle reaches of the Tururе clustered with the Caroni drainage

317 (Willing et al. 2010), and more recent marker-based studies distinguishing local from invasive individuals
318 demonstrated that the invasion extended to, or beyond, the Tururе–Quare confluence (Sievers et al. 2012).
319 Continuous migration from above the barrier due to stochastic events such as flooding, together with
320 subsequent effective mixing might explain this pattern (Sievers et al. 2012). However, the rapidity of the
321 replacement of native fish in the downstream population, despite their larger effective population sizes,
322 suggests that additional factors might have contributed to the success of the invaders. If so, the translocation
323 experiment—designed to test the adaptive potential of guppies in novel environments—may ultimately have
324 facilitated the loss of multiple populations within the drainage that were genetically distinct from guppies in
325 other systems (Sievers et al. 2012).

326 The absence of strong geographic barriers in the lower Oropouche drainage likely promotes gene flow, which
327 is particularly evident in the Quare population and, to a lesser extent, in La Seiva (Fig. 1A). However, our
328 analyses revealed no evidence of Tururе ancestry in the lower Quare or La Seiva populations (Fig. 1A),
329 consistent with findings ~15 years earlier (Willing et al. 2010). Nonetheless, the Tururе invasion proceeded
330 rapidly, and our results suggest that the initial bottleneck—by increasing the efficiency of purging strongly
331 deleterious mutations—may have contributed to this successful colonization. Other studies of bottlenecked
332 vertebrate populations have yielded mixed conclusions ranging from no evidence of purging at all (Robinson
333 et al. 2019; Ochoa et al. 2022; Smeds et al. 2024), purging of only the most deleterious class of mutations
334 (Grossen et al. 2020; Khan et al. 2021; Quinn et al. 2024), or accumulation of all classes of deleterious
335 mutations (van der Valk et al. 2019). Disentangling whether such variation reflects methodological differences,
336 limited statistical power, annotation quality, or true evolutionary processes remains difficult (Quinn et al.
337 2024). One critical factor may be the strength and duration of the bottleneck. Theory predicts that purging is
338 most efficient under moderate reductions in population size, which expose recessive deleterious alleles to
339 selection yet still allow selection to overcome genetic drift (Crow 1970; Glémin 2003; Robinson et al. 2023;
340 Lombaert et al. 2025). Consistent with this, Quinn et al. (2024), found evidence of purging of loss-of-function
341 alleles in populations that experienced less severe size declines, whereas populations undergoing the most
342 rapid and drastic bottlenecks showed weaker signals of purging. This pattern suggests that extinction risk is
343 the highest in severely reduced populations, where purging is the least effective. Our results align with these
344 expectations. In the Tururе River, the translocated population does not show a marked reduction in estimated

345 neutral diversity or increase in Tajima's D values, compared with its progenitor (Fig. 2, Supplemental Fig. S1).
346 This likely reflects the moderate severity of the bottleneck and the relatively large number of individuals
347 introduced (see Introduction; (Shaw et al. 1992; Sievers et al. 2012)). Despite these subtle changes, we
348 nevertheless detect pronounced shifts in the genetic load estimates, supporting the view that purging can be
349 effective under moderate bottlenecks.

350 ***Admixture reshapes the landscape of genetic load in an expanding population***

351 Our investigation of the Turure expansion gradient revealed that total RGL and RML decline further
352 downstream (Fig. 5), which could, in principle, reflect repeated purging events following successive
353 bottlenecks. However, this would cause a gradual loss of nucleotide diversity and a depletion of rare variants,
354 while purging should primarily reduce heterozygous load by targeting the most deleterious mutations. In
355 contrast, we found increased nucleotide diversity and lower Tajima's D values in the middle and lower Turure
356 populations compared with the up-river population. Moreover, the decline in genetic load is driven mainly by
357 reductions in homozygous load, whereas heterozygous load remains largely unchanged or only moderately
358 affected. Strikingly, for the most deleterious loss-of-function alleles, genetic load actually increases rather than
359 decreases.

360 We therefore suggest that changes in genetic load along the Turure River primarily reflect admixture occurring
361 below the waterfall barrier in the middle and lower reaches of the river. The upper and lower populations
362 indeed differ substantially in their genetic composition, with the lower populations showing pronounced
363 admixture with other ancestries (Fig. 1A). Depending on the genetic makeup of the admixed sources and the
364 degree of divergence between them, such admixture could have profoundly reshaped the landscape of genetic
365 load by increasing the heterozygote frequencies and introducing new haplotypes into the population.

366 Our analyses revealed a strong correlation between total RGL and long-term effective population size, as
367 inferred from neutral nucleotide diversity (Fig. 3). Rivers in the Oropouche drainage generally exhibit higher
368 nucleotide diversity than those in the Caroni drainage (Fig. 2), suggesting that a lower total RGL should be
369 expected in Oropouche populations. This pattern is also supported in our comparisons of total RGL between
370 the two drainages (Supplemental Table S5). If the native Turure ancestry from the Oropouche drainage
371 followed this trend, it would have carried fewer moderately deleterious mutations than the Caroni guppies

introduced during translocation. Consequently, admixture between these ancestries should, on average, reduce the genetic load of the expanding population consistent with our observations. As expected, this reduction in total RGL (and similarly in total RML) is driven primarily by decreases in homozygous load, likely reflecting the masking of moderately deleterious alleles that became fixed in the Caroni lineage after the Caroni-Oropouche divergence.

The most deleterious LoF mutations should rarely be fixed in unthreatened natural populations. Our neutral diversity dataset did not predict changes in RLL, suggesting that strongly deleterious mutations segregate and fix at comparable rates in different guppy populations (except for the purging in the Tururе upriver population explained above). We also detected no significant difference in RLL between the Oropouche and Caroni drainages (Supplemental Tab. S5). Admixture is therefore the most likely explanation for an increase in RLL in the lower compared to upper Tururе, which likely counteracted purging by increasing heterozygosity, at the same time introducing new deleterious mutations from an unpurged native Tururе population (Fig. 5).

Overall, our results indicate that the recently translocated guppy population purged strongly deleterious mutations during the bottleneck, while the genetic load has been largely reestablished by subsequent mixing with local populations along the expansion gradient. Invader populations can thus exhibit a reshaped landscape of genetic load, with both population size reductions and admixture exerting significant influence on these patterns. These findings are relevant to understanding genetic processes in invasive species, which in a globally connected world are recognized as one of the major threats to biodiversity (Faulkner et al. 2024; Wallingford et al. 2020). Although biologists have long proposed that evolutionary processes play a key role in invasion success (Estoup et al. 2016), it is only recently that the abundance of deleterious alleles has been considered. Our results highlight that while deleterious alleles accumulate over thousands of generations (Wootton et al. 2023; van der Valk et al. 2019), they can be rapidly redistributed through genetic drift, selection, and gene flow when populations mix. Yet, it should be stressed that our analyses did not take into account several processes which may affect our interpretation, such as epistatic interactions, and local adaptation resulting from different environmental pressures encountered by the different populations we sampled. We emphasize that our study is correlational, and future studies should attempt to investigate the fitness consequences of the inferred genetic load. Furthermore, the temporal scope of our study reflects a relatively recent population expansion, and the long-term consequences of such demographic processes may differ over extended evolutionary timescales.

400 Despite these limitations, our results highlight that admixture and biological invasions are associated with
401 important consequences for genetic load segregating in populations.

402

403 **METHODS**

404 ***Sampling and sequencing***

405 Individuals used in the study come from two batches of sampling and sequencing supplemented with 10
406 samples (Guanapo lower population) downloaded from the European Nucleotide Archive BioProject
407 PRJEB10680. The first batch (51 individuals) of sampling was conducted in 2018 and sequenced in 2019. The
408 second batch (140 individuals) was both sampled and sequenced in 2022. All individuals are wild fish from
409 natural populations in Trinidad and Tobago. The sampling procedures complied with Polish law, European
410 Directive 2010/63/EU and were conducted under permits issued by Ministry of Agriculture, Land and Fisheries
411 of Trinidad and Tobago.

412 We sampled eight rivers on Trinidad - Aripo, Caura, Lopinot, and Santa Cruz (Caroni drainage), as well as La
413 Seiva, Oropouche, Quare and Turure (Oropouche drainage) - and two rivers on Tobago: Dog River and
414 Roxborough, collecting 191 individuals from 14 sampling locations/populations in total. Three rivers were
415 sampled at multiple sites: Quare (upper and lower), Oropouche (upper and lower), and Turure (upper, middle
416 and lower); see Fig 1B and Supplemental Table S1 for more details and geographic coordinates. Fish were
417 anesthetized using tricaine mesylate (MS-222) and preserved in 98% ethanol. Tail fin tissue was used for DNA
418 extraction (with Thermo Scientific™ MagJET™ Genomic DNA kit) and genomic libraries generation (with
419 the NEBNext Ultra™ II FS DNA Library Prep Kit and NEBNext Multiplex Oligos for Illumina indices)
420 according to manufacturer protocols. All samples were sequenced on the Illumina NovaSeq 6000 platform in
421 2x150bp mode at the NGI Sweden. Together with the ENA archive Guanapo samples, 201 samples from 15
422 populations were included for subsequent analyses.

423 ***Population structure and nucleotide diversity***

Raw sequencing reads were filtered with Trimmomatic (version 0.39; (Bolger et al. 2014)) and aligned to the guppy female reference genome (GCF_000633615.2; (Kunstner et al. 2016)) using bwa mem and default parameters (v0.7.10; (Li 2013)). The resulting BAM files were then subjected to duplicate marking with Picard tools (v2.21.6; http://broadinstitute.github.io/picard/). One sample from lower Oropouche had low mean coverage and was excluded from further analyses leaving, 200 samples in total.

To characterize the genetic composition of the samples, we performed principal component analysis (PCA) and ancestry inference. First, we jointly called variants in all BAM files using samtools mpileup (with -a AD parameter; v1.20, (Danecek et al. 2021)) and bcftools call (with -G populations indicating parameter and -m multiallelic parameter; v1.20) Resulting VCF was then filtered with bcftools (version 0.1.12b, (Danecek et al. 2011)) using the following thresholds: MapppingQuality > 40, INFO/Depth < 5200, INFO/Depth > 1300, QUAL ≥ 30, MappingQualityBias > -3, ReadPositionBias < 3, SoftClipLengthBias < 3; and with vcftools (v0.1.12b, Danecek et al. 2011): MinorAlleleFraction ≥ 0.01, MaxAlelles = 2, MaxMissing = 50%; Depth ≥ 6 and GenotypeQuality ≥ 70. We then used plink (v1.9; (Purcell et al. 2007)) to transform the VCF file into a BED file and to prune it for variants in linkage disequilibrium using 200bp window, 1bp step and 0.5 r^2 threshold. The resulting BED file was used to perform PCA. Using the same BED file, we ran Admixture (with the -s random seed parameter; v1.3, (Alexander et al. 2009)) 10 times for each K parameter (1-15). The Admixture results were plotted with Pong software (with -s 0.95 threshold to combine similar clusters at given K; v1.5, (Behr et al. 2016)).

To calculate neutral nucleotide diversity in our populations, we first identified fourfold-degenerated sites in the guppy genome using the find_4fds script (GitHub: https://github.com/mattheatley/extract_4fds). We then called genotypes in our samples using the same approach as above, including both polymorphic and monomorphic sites. The resulting VCF file was filtered with bcftools (v0.1.12b) as follows: MapppingQuality > 40, INFO/Depth < 5200, INFO/Depth > 1300, QUAL ≥ 30 and with vcftools (v0.1.12b): MaxAlelles = 2, MaxMissing = 50%; Depth ≥ 6 and retained only those that were located in 4-fold degenerated sites. Resulting files were used to calculate nucleotide diversity (π) in 1Mb windows across the genome with the Pixy tool (v1.2.7.beta1; (Korunes and Samuk 2021)). To estimate uncertainty around nucleotide diversity, we implemented a custom Python script that reproduced the estimator used in Pixy. For each population, individuals were resampled with replacement from the VCF genotype matrix, and nucleotide diversity was

452 recalculated for each bootstrap replicate using the same pairwise comparison framework and missing-data
453 handling as implemented in Pixy. This procedure was repeated 100 times to generate a bootstrap distribution
454 of π estimates, from which the variance around the genome-wide estimate was derived.

455 ***Ancestral allele inference and Conservation Scores***

456 To infer guppy ancestral alleles (AA) we followed the approach of Smeds et al. (2024) and used genomic
457 information from two closely related outgroups: *Micropoecilia picta* and *Xiphophorus maculatus*. Sequencing
458 data for these two species were retrieved from NCBI's SRA (accession numbers: ERR4077394 and
459 SRR13649980, respectively) in FASTQ format. Reads were mapped to the guppy female reference genome
460 and genotype calling was performed as described above, producing whole-genome VCF files These files were
461 then used in the pseudo_haploidize.py script by Smeds et al. (2023, GitHub: https://github.com/linneas/wolf-
462 deleterious) to infer ancestral alleles based on allele depth weight. Minimum depth thresholds were set to half
463 of the expected coverage of *X. maculatus* and *M. picta* (7 and 11 respectively), and the minimum genotype
464 quality was set to 30. Haplotypes that did not meet these thresholds were coded as "N". The two resulting BED
465 files (one per species) were merged and only sites where the nucleotide was identical for both species (and not
466 N) were retained as informative for ancestral allele inference.

467 To obtain conservation scores (CS), we downloaded the CS BED file from the Ensembl fish Compara database
468 (release 111, 65 fish species alignment, CS calculated with GERP, (Herrero et al. 2016)). Briefly, GERP
469 quantifies evolutionary constraint by estimating the number of rejected substitutions at each alignment
470 position. This is achieved by comparing the observed substitution rate to that expected under a neutral
471 phylogenetic model inferred from the multiple sequence alignment. Positive GERP scores indicate sites under
472 purifying selection (fewer substitutions than expected), whereas negative scores indicate an excess of
473 substitutions relative to neutrality. The file was intersected with the ancestral allele BED file. The resulting
474 CS-AA BED was used for genotype filtering, as described below.

475 ***Genetic Load estimation***

476 To estimate genetic load, we developed a bioinformatic pipeline analyzing within-population genomic
477 variation. Each population was analyzed separately, enabling parallelization and the detection of rare variants.

First, we inferred genotypes with GATK HaplotypeCaller (with `-ERC BP_RESOLUTION` and `--output-mode EMIT_ALL_CONFIDENT_SITES` parameters, v4.1.4.1; (McKenna et al. 2010)). Single individual genomic VCF (GVFCs) files were merged into population GVCFs (GATK CombineGVCFs) and used in GATK GenotypeGVCFs to produce VCF files in all-sites mode (`-all-sites`). Sites with fewer than 70% of genotypes meeting quality thresholds (DP ≥ 6 and GQ ≥ 30) were removed. Subsequently, we filtered out multiallelic sites and retained only sites with both CS and AA as one of the two alleles. Information about CS and AA was added to the INFO field using a custom Python script. In case of sites, where AA was the alternative to the reference nucleotide, the two alleles were swapped, so that REF always represents the ancestral allele in the final VCF file.

Because our samples differed in expected coverage, we applied individual-depth-based filtering. Only genotypes meeting the criteria 2 × mean DP of the individual ≥ DP ≥ 6 and GQ ≥ 30 were retained; genotypes failing these thresholds were coded as missing. Sites with more than 30% missing genotypes were excluded. Finally we extracted SNPs and removed variants failing GATK-recommended quality filters: QualityByDepth ≥ 2, MappingQuality ≥ 40, FisherScore ≤ 60, StrandOddsRatio ≤ 3, MappingQualityRankSum ≥ −12.5, ReadPosRankSum ≥ −8.

Per-individual relative genetic load (RGL) was calculated following the approach of Dussex et al. (2021), using the following formula:

$$RGL = \frac{\sum_{\substack{i=1 \\ CS_i \geq 2}}^{n} CS_i \cdot D_i}{\sum_{i=1}^{n} D_i}$$

where n is the number of variants, CS_i is the conservation score and D_i is the number of derived alleles of the ith variant. Only alleles at highly conserved sites (conservation score ≥ 2) were included in the numerator.

Additionally, we used called SNPs to identify loss of function (LOF, nonsense), missense and synonymous variants with SNPEff tool (v5.0; (Cingolani et al. 2012)) using built-in annotation originated from ensemble release 99. The values were calculated and normalized against synonymous derived alleles to calculate relative LOF load (RLL) using the following formulas:

502 $$RLL = \frac{\sum^{n}_{\substack{i=1 \\ t \in LOF}} D_i}{\sum^{n}_{\substack{i=1 \\ t \in syn}} D_i}$$

503 where n is the number of variants, t is the variant type and D_i is the number of derived alleles of the ith variant.

504 Similarly, values for missense alleles were also used to calculate relative missense load (RML) using the
505 following formula:

506 $$RML = \frac{\sum^{n}_{\substack{i=1 \\ t \in mis}} D_i}{\sum^{n}_{\substack{i=1 \\ t \in syn}} D_i}$$

507 where n is the number of variants, t is the variant type and D_i is the number of derived alleles of the ith variant.

508 The calculations were done separately for all variants (as a proxy for total genetic load), heterozygous
509 genotypes (heterozygous genetic load) and homozygous genotypes (homozygous genetic load).

510 ***Statistical analyses***

511 All statistical analyses were performed in R (v4.5.3) Model assumptions were verified by examining diagnostic
512 plots of residuals (or simulated residuals where appropriate) using the DHARMa package (Hartig 2016).

513 The association between mutation load and nucleotide diversity, was tested using general or generalized linear
514 models, with a Gaussian distribution for RGL, and binomial distribution for RML and RLL. A logarithmic
515 transformation was used to address the detected heteroskedasticity (reported in Supplemental Table S6). We
516 initially fitted geographic region (Caroni, Oropuche, Tobago) in this model along with population, but the
517 region was not significant in any analysis and some models containing it did not conform to model assumptions
518 (heteroskedasticity), which improved when the region was removed. Therefore, we removed the region from
519 all models.

520 We used general or generalized linear mixed models using glmmTMB package to compare genetic load
521 between region, with population as a random effect and coverage as a covariate. We used a Gaussian
522 distribution for RGL, and a binomial distribution for RML and RLL. We compared populations within Turure,

between Tururе and Guanapo and between the upper and lower parts of streams within Oropuche using general (RGL) or generalized (RGL and RLL) linear models. These models included coverage as a covariate and batch as a fixed effect (except for the Tururе and Guanapo comparison, in which batch and population effects could not be differentiated). For the generalized models, we used a binomial distribution, or, when over- or underdispersion was detected, a quasibinomial distribution (in which case we report the dispersion parameter, Supplemental Tab. S7 – S9). In our analysis of the differences between regions (Supplemental Tab. S5) in nucleotide diversity (Supplemental Tab. S6), only the lower river sites were used and all Tururе populations were excluded.

Declaration of generative AI in the writing process

During the preparation of this manuscript we used ChatGPT to improve the language and clarity of the text. Authors reviewed and edited the content after using this tool, and take full responsibility for the final version of the manuscript.

DATA ACCESS

All raw sequencing data generated in this study have been submitted to the NCBI Short Read Archive under accession number PRJNA1040274.

All codes are available in a GitHub repository (https://github.com/0-Ioniel-0/Expansion_Load) and in the Supplemental Code.

COMPETING INTEREST STATEMENT

The authors declare no competing interests.

ACKNOWLADGMENTS

We are grateful to Deborah Charlesworth, Wiesław Babik and Jonathan Parrett for their valuable comments on an early version of the manuscript, and to the members of the Evolutionary Biology Group for their insightful discussions and continuous support. We thank Katarzyna Dudek from Jagiellonian University for preparing genomic libraries. This work was funded by the Polish National Science Centre 2018/31/D/NZ8/00091 grant. M.K. was supported by the Polish National Agency for Academic Exchange under the Bekker Programme.

Computations were performed at the Poznan Supercomputing and Networking Centre. We are also grateful to the Fisheries Division of the Ministry of Agriculture and Fisheries, Republic of Trinidad and Tobago for granting permission to collect and export of fish tissue.

FIGURE LEGENDS

Figure 1. Genetic structure of the analysed dataset. (A) Admixture plots from analyses with optimal values of K (12). The regions are color-coded in the strip above the plots as follows: Tobago - dark blue, Caroni drainage - light blue, Oropouche drainage - green, and Turure - red. Grey triangle below the Admixture plot points to individuals of unknown origin, excluded from the analyses. (**B)** Sampling locations in Trinidad and Tobago, across the rivers: SCR (Santa Cruz), CAU (Caura), LOP (Lopinot), ARI (Aripo), Guanapo (GUA), QUA (Quare), TUR (Turure), LSA (La Seiva), ORO (Oropouche), DR (Dog River), ROX (Roxborough). **(C)** Principal Component Analysis of guppy populations based on genome-wide variation. Each point is one individual.

Figure 2. Nucleotide diversity (π) at fourfold degenerate sites across the analyzed populations. Estimates were obtained by bootstrapping individuals within each population. Bars represent the median π across 100 bootstrap replicates, and whiskers indicate the 95% bootstrap interval (2.5–97.5%). Populations are color-coded by region: Tobago (dark blue), Caroni drainage (light blue), Oropouche drainage (green), and Turure (red).

Figure 3. The relationship between neutral nucleotide diversity (calculated in four-fold degenerated sites) and per-population estimates of relative genetic load averaged within populations.

Figure 4. Comparisons of load estimates between Guanapo and upper Turure – pre- and post-translocation populations respectively. The top panel represents relative genetic load (RGL), the middle panel relative loss-of-function load (RLL) and the bottom panel relative missense load (RML). Boxplots are drawn from individual-based estimates with the horizontal line representing the population median, the boxes the interquartile range and the whiskers the maximum and minimum values. Horizontal lines with asterisks indicate statistically significant differences.

578

579 **Figure 5. Comparisons of load estimates between the upper, middle and lower sites in the Tururе river.**
580 The top panel shows relative genetic load (RGL), the middle panel shows relative loss-of-function load (RLL)
581 and the bottom panel shows relative missense load (RML). Boxplots drawn from individual-based estimates
582 with horizontal lines representing the population median, boxes the interquartile range, and whiskers the
583 maximum and minimum values. Horizontal lines with asterisks indicate statistically significant differences.

584

585 **REFERENCES**

586 Alexander DH, Novembre J, Lange K. 2009. Fast model-based estimation of ancestry in unrelated
587 individuals. *Genome Res* **19**: 1655–1664.

588 Avsec Ž, Latysheva N, Cheng J, Novati G, Taylor KR, Ward T, Bycroft C, Nicolaisen L, Arvaniti
589 E, Pan J. 2025. AlphaGenome: advancing regulatory variant effect prediction with a unified
590 DNA sequence model. *BioRxiv* 2006–2025.

591 Barker BS, Cocio JE, Anderson SR, Braasch JE, Cang FA, Gillette HD, Dlugosch KM. 2019.
592 Potential limits to the benefits of admixture during biological invasion. *Mol Ecol* **28**: 100–113.

593 Barrett SCH, Charlesworth D. 1991. Effects of a change in the level of inbreeding on the genetic
594 load. *Nature* **352**: 522–524.

595 Bassar RD, Marshall MC, López-Sepulcre A, Zandonà E, Auer SK, Travis J, Pringle CM, Flecker
596 AS, Thomas SA, Fraser DF. 2010. Local adaptation in Trinidadian guppies alters ecosystem
597 processes. *Proc Natl Acad Sci* **107**: 3616–3621.

598 Becher SA, Magurran AE. 2000. Gene flow in Trinidadian guppies. *J Fish Biol* **56**: 241–249.

599 Behr AA, Liu KZ, Liu-Fang G, Nakka P, Ramachandran S. 2016. Pong: fast analysis and
600 visualization of latent clusters in population genetic data. *Bioinformatics* **32**: 2817–2823.

601 Bertorelle G, Raffini F, Bosse M, Bortoluzzi C, Iannucci A, Trucchi E, Morales HE, van Oosterhout
602 C. 2022. Genetic load: genomic estimates and applications in non-model animals. *Nat Rev*

603 *Genet* **23**: 492–503.
604 Bolger AM, Lohse M, Usadel B. 2014. Trimmomatic: A flexible trimmer for Illumina sequence
605 data. *Bioinformatics* **30**: 2114–2120.
606 Caballero A, Bravo I, Wang J. 2017. Inbreeding load and purging: implications for the short-term
607 survival and the conservation management of small populations. *Heredity (Edinb)* **118**: 177–
608 185.
609 Charlesworth D, Willis JH. 2009. The genetics of inbreeding depression. *Nat Rev Genet* **10**: 783–
610 796.
611 Cheng J, Novati G, Pan J, Bycroft C, Žemgulytė A, Applebaum T, Pritzel A, Wong LH, Zielinski
612 M, Sargeant T. 2023. Accurate proteome-wide missense variant effect prediction with
613 AlphaMissense. *Science (80-)* **381**: eadg7492.
614 Cingolani P, Platts A, Wang LL, Coon M, Nguyen T, Wang L, Land SJ, Lu X, Ruden DM. 2012. A
615 program for annotating and predicting the effects of single nucleotide polymorphisms, SnpEff:
616 SNPs in the genome of Drosophila melanogaster strain w1118; iso-2; iso-3. *Fly (Austin)* **6**: 80–
617 92.
618 Colautti RI, Alexander JM, Dlugosch KM, Keller SR, Sultan SE. 2017. Invasions and extinctions
619 through the looking glass of evolutionary ecology. *Philos Trans R Soc B Biol Sci* **372**:
620 20160031.
621 Crnokrak P, Barrett SCH. 2002. Perspective: purging the genetic load: a review of the experimental
622 evidence. *Evolution (N Y)* **56**: 2347–2358.
623 Crow JF. 1970. Genetic loads and the cost of natural selection. In *Mathematical topics in*
624 *population genetics*, pp. 128–177, Springer.
625 Crow JF. 1989. Some possibilities for measuring selection intensities in man. *Hum Biol* **61**: 763–
626 775.
627 Danecek P, Auton A, Abecasis G, Albers CA, Banks E, DePristo MA, Handsaker RE, Lunter G,
628 Marth GT, Sherry ST, et al. 2011. The variant call format and VCFtools. *Bioinformatics* **27**:

2156–2158.

Danecek P, Bonfield JK, Liddle J, Marshall J, Ohan V, Pollard MO, Whitwham A, Keane T, McCarthy SA, Davies RM. 2021. Twelve years of SAMtools and BCFtools. *Gigascience* **10**: giab008.

Davydov E V, Goode DL, Sirota M, Cooper GM, Sidow A, Batzoglou S. 2010. Identifying a high fraction of the human genome to be under selective constraint using GERP++. *PLoS Comput Biol* **6**: e1001025.

de Pedro M, Riba M, González-Martínez SC, Seoane P, Bautista R, Claros MG, Mayol M. 2021. Demography, genetic diversity and expansion load in the colonizing species Leontodon longirostris (Asteraceae) throughout its native range. *Mol Ecol* **30**: 1190–1205.

Deacon AE, Ramnarine IW, Magurran AE. 2011. How reproductive ecology contributes to the spread of a globally invasive fish. *PLoS One* **6**: e24416.

Devigili A, Fitzpatrick JL, Gasparini C, Ramnarine IW, Pilastro A, Evans JP. 2018. Possible glimpses into early speciation: The effect of ovarian fluid on sperm velocity accords with post-copulatory isolation between two guppy populations. *J Evol Biol* **31**: 66–74.

DeWoody JA, Harder AM, Mathur S, Willoughby JR. 2021. The long-standing significance of genetic diversity in conservation. *Mol Ecol* **30**: 4147–4154.

Dussex N, Morales HE, Grossen C, Dalén L, van Oosterhout C. 2023. Purging and accumulation of genetic load in conservation. *Trends Ecol Evol* **38**: 961–969.

Dussex N, Van Der Valk T, Morales HE, Wheat CW, Díez-del-Molino D, Von Seth J, Foster Y, Kutschera VE, Guschanski K, Rhie A. 2021. Population genomics of the critically endangered kākāpō. *Cell Genomics* **1**.

Endler JA. 1980. Natural Selection on Color Patterns in Poecilia reticulata. *Evolution (N Y)*.

Estoup A, Ravigné V, Hufbauer R, Vitalis R, Gautier M, Facon B. 2016. Is there a genetic paradox of biological invasion? *Annu Rev Ecol Evol Syst* **47**: 51–72.

Eyre-Walker A, Keightley PD. 2007. The distribution of fitness effects of new mutations. *Nat Rev*

655 *Genet* **8**: 610–618.
656 Facon B, Hufbauer RA, Tayeh A, Loiseau A, Lombaert E, Vitalis R, Guillemaud T, Lundgren JG,
657 Estoup A. 2011. Inbreeding depression is purged in the invasive insect Harmonia axyridis.
658 *Curr Biol* **21**: 424–427.
659 Fajen A, Breden F. 1992. Mitochondrial DNA sequence variation among natural populations of the
660 Trinidad guppy, Poecilia reticulata. *Evolution (N Y)* **46**: 1457–1465.
661 Faulkner KT, Hulme PE, Wilson JRU. 2024. Harder, better, faster, stronger? Dispersal in the
662 Anthropocene. *Trends Ecol Evol* **39**: 1130–1140.
663 Fitzpatrick SW, Gerberich JC, Angeloni LM, Bailey LL, Broder ED, Torres-Dowdall J,
664 Handelsman CA, López-Sepulcre A, Reznick DN, Ghalambor CK. 2016. Gene flow from an
665 adaptively divergent source causes rescue through genetic and demographic factors in two wild
666 populations of T rinidadian guppies. *Evol Appl* **9**: 879–891.
667 Fraser BA, Künstner A, Reznick DN, Dreyer C, Weigel D. 2015. Population genomics of natural
668 and experimental populations of guppies (Poecilia reticulata). *Mol Ecol* **24**: 389–408.
669 García-Dorado A. 2012. Understanding and predicting the fitness decline of shrunk populations:
670 inbreeding, purging, mutation, and standard selection. *Genetics* **190**: 1461–1476.
671 Glémin S. 2003. How are deleterious mutations purged? Drift versus nonrandom mating. *Evolution*
672 *(N Y)* **57**: 2678–2687.
673 Grossen C, Guillaume F, Keller LF, Croll D. 2020. Purging of highly deleterious mutations through
674 severe bottlenecks in Alpine ibex. *Nat Commun* **11**: 1001.
675 Harris K, Nielsen R. 2016. The genetic cost of Neanderthal introgression. *Genetics* **203**: 881–891.
676 Hartig F. 2016. DHARMa: residual diagnostics for hierarchical (multi-level/mixed) regression
677 models. *CRAN Contrib Packag*.
678 Herrero J, Muffato M, Beal K, Fitzgerald S, Gordon L, Pignatelli M, Vilella AJ, Searle SMJ,
679 Amode R, Brent S. 2016. Ensembl comparative genomics resources. *Database* **2016**: bav096.
680 Johnson CN, Balmford A, Brook BW, Buettel JC, Galetti M, Guangchun L, Wilmshurst JM. 2017.

681 Biodiversity losses and conservation responses in the Anthropocene. *Science (80-)* **356**: 270–
682 275.
683 Karczewski KJ, Francioli LC, Tiao G, Cummings BB, Alföldi J, Wang Q, Collins RL, Laricchia
684 KM, Ganna A, Birnbaum DP. 2020. The mutational constraint spectrum quantified from
685 variation in 141,456 humans. *Nature* **581**: 434–443.
686 Kardos M, Armstrong EE, Fitzpatrick SW, Hauser S, Hedrick PW, Miller JM, Tallmon DA, Funk
687 WC. 2021. The crucial role of genome-wide genetic variation in conservation. *Proc Natl Acad*
688 *Sci* **118**: e2104642118.
689 Kardos M, Keller LF, Funk WC. 2025. What can genome sequence data reveal about population
690 viability? *Mol Ecol* **34**: e17608.
691 Kardos M, Zhang Y, Parsons KM, Kang H, Xu X, Liu X, Matkin CO, Zhang P, Ward EJ, Hanson
692 MB. 2023. Inbreeding depression explains killer whale population dynamics. *Nat Ecol Evol* **7**:
693 675–686.
694 Keller LF, Waller DM. 2002. Inbreeding effects in wild populations. *Trends Ecol Evol* **17**: 230–
695 241.
696 Kemp DJ, Batistic F-K, Reznick DN. 2018. Predictable adaptive trajectories of sexual coloration in
697 the wild: evidence from replicate experimental guppy populations. *Evolution (N Y)* **72**: 2462–
698 2477.
699 Khan A, Patel K, Shukla H, Viswanathan A, van der Valk T, Borthakur U, Nigam P, Zachariah A,
700 Jhala Y V, Kardos M. 2021. Genomic evidence for inbreeding depression and purging of
701 deleterious genetic variation in Indian tigers. *Proc Natl Acad Sci* **118**: e2023018118.
702 Kimura M, Maruyama T, Crow JF. 1963. The mutation load in small populations. *Genetics* **48**:
703 1303.
704 Kimura M, Ohta T. 1969. The average number of generations until fixation of a mutant gene in a
705 finite population. *Genetics* **61**: 763.
706 Kleinman-Ruiz D, Lucena-Perez M, Villanueva B, Fernández J, Saveljev AP, Ratkiewicz M,

Schmidt K, Galtier N, García-Dorado A, Godoy JA. 2022. Purging of deleterious burden in the endangered Iberian lynx. *Proc Natl Acad Sci* **119**: e2110614119.

Kołodziejczyk J, Fijarczyk A, Porth I, Robakowski P, Vella N, Vella A, Kloch A, Biedrzycka A. 2025. Genomic investigations of successful invasions: the picture emerging from recent studies. *Biol Rev* **100**: 1396–1418.

Korunes KL, Samuk K. 2021. pixy: Unbiased estimation of nucleotide diversity and divergence in the presence of missing data. *Mol Ecol Resour* **21**: 1359–1368.

Kuang W, Hu J, Wu H, Fen X, Dai Q, Fu Q, Xiao W, Frantz L, Roos C, Nadler T. 2020. Genetic diversity, inbreeding level, and genetic load in endangered snub-nosed monkeys (Rhinopithecus). *Front Genet* **11**: 615926.

Kunstner A, Hoffmann M, Fraser BA, Kottler VA, Sharma E, Weigel D, Dreyer C. 2016. The genome of the trinidadian guppy, Poecilia reticulata, and variation in the Guanapo population. *PLoS One* **11**: e0169087.

Kyriazis CC, Wayne RK, Lohmueller KE. 2021. Strongly deleterious mutations are a primary determinant of extinction risk due to inbreeding depression. *Evol Lett* **5**: 33–47. https://onlinelibrary.wiley.com/doi/full/10.1002/evl3.209 (Accessed July 8, 2021).

Lan T, Li H, Liu B, Shi M, Tian Y, Sahu SK, Cui L, Dussex N, Liu D, Ma Y. 2025. Revealing extensive inbreeding and less efficient purging of deleterious mutations in wild Amur tigers in China. *J Genet Genomics* **52**: 641–649.

Lande R. 1998. Risk of population extinction from fixation of deleterious and reverse mutations. *Genetica* **102**: 21–27.

Li H. 2013. Aligning sequence reads, clone sequences and assembly contigs with BWA-MEM. *arXiv Prepr arXiv* **00**: 3. http://arxiv.org/abs/1303.3997.

Lindholm AK, Breden F, Alexander HJ, CHAN W, Thakurta SG, Brooks R. 2005. Invasion success and genetic diversity of introduced populations of guppies Poecilia reticulata in Australia. *Mol Ecol* **14**: 3671–3682.

733 Lombaert E, Blin A, Porro B, Guillemaud T, Bernal JS, Chang G, Kirichenko N, Sappington TW,
734 Toepfer S, Deleury E. 2025. Unraveling genetic load dynamics during biological invasion:
735 insights from two invasive insect species. *Peer Community J* **5**.
736 Lynch M, Conery J, Burger R, Lande R. 1995. Mutation accumulation and the extinction of small
737 populations. *Science (80-)* **146**: 1455–1460.
738 Magurran AE. 2005. *Evolutionary ecology: the Trinidadian guppy*.
739 Mathur S, DeWoody JA. 2021. Genetic load has potential in large populations but is realized in
740 small inbred populations. *Evol Appl* **14**: 1540–1557.
741 Mathur S, Mason AJ, Bradburd GS, Gibbs HL. 2023a. Functional genomic diversity is correlated
742 with neutral genomic diversity in populations of an endangered rattlesnake. *Proc Natl Acad Sci*
743 **120**: e2303043120.
744 Mathur S, Tomeček JM, Tarango-Arámbula LA, Perez RM, DeWoody JA. 2023b. An evolutionary
745 perspective on genetic load in small, isolated populations as informed by whole genome
746 resequencing and forward-time simulations. *Evolution (N Y)* **77**: 690–704.
747 McKenna A, Hanna M, Banks E, Sivachenko A, Cibulskis K, Kernytsky A, Garimella K, Altshuler
748 D, Gabriel S, Daly M, et al. 2010. The Genome Analysis Toolkit: A MapReduce framework
749 for analyzing next-generation DNA sequencing data. *Genome Res* **20**: 1297–1303.
750 Ochoa A, Gibbs HL. 2021. Genomic signatures of inbreeding and mutation load in a threatened
751 rattlesnake. *Mol Ecol* **30**: 5454–5469.
752 Ochoa A, Onorato DP, Roelke-Parker ME, Culver M, Fitak RR. 2022. Give and take: Effects of
753 genetic admixture on mutation load in endangered Florida panthers. *J Hered* **113**: 491–499.
754 Peischl S, Kirkpatrick M, Excoffier L. 2015. Expansion load and the evolutionary dynamics of a
755 species range. *Am Nat* **185**: E81–E93.
756 Purcell S, Neale B, Todd-Brown K, Thomas L, Ferreira MAR, Bender D, Maller J, Sklar P, de
757 Bakker PIW, Daly MJ, et al. 2007. PLINK: a tool set for whole-genome association and
758 population-based linkage analyses. *Am J Hum Genet* **81**: 559–575.

759 Qiu S, Yong L, Wilson A, Croft DP, Graham C, Charlesworth D. 2022. Partial sex linkage and
760 linkage disequilibrium on the guppy sex chromosome. *Mol Ecol* **31**: 5524–5537.
761 Quinn CB, Preckler-Quisquater S, Buchalski MR, Sacks BN. 2024. Whole genomes inform genetic
762 rescue strategy for montane red foxes in North America. *Mol Biol Evol* **41**: msae193.
763 Ralls K, Sunnucks P, Lacy RC, Frankham R. 2020. Genetic rescue: A critique of the evidence
764 supports maximizing genetic diversity rather than minimizing the introduction of putatively
765 harmful genetic variation. *Biol Conserv* **251**: 108784.
766 Reznick DA, Bryga H, Endler JA. 1990. Experimentally induced life-history evolution in a natural
767 population. *Nature* **346**: 357–359.
768 Reznick DN, Bryga H. 1987. Life-history evolution in guppies (Poecilia reticulata): 1. Phenotypic
769 and genetic changes in an introduction experiment. *Evolution (N Y)* **41**: 1370–1385.
770 Robinson J, Kyriazis CC, Yuan SC, Lohmueller KE. 2023. Deleterious variation in natural
771 populations and implications for conservation genetics. *Annu Rev Anim Biosci* **11**: 93–114.
772 Robinson JA, Brown C, Kim BY, Lohmueller KE, Wayne RK. 2018. Purging of strongly
773 deleterious mutations explains long-term persistence and absence of inbreeding depression in
774 island foxes. *Curr Biol* **28**: 3487–3494.
775 Robinson JA, Räikkönen J, Vucetich LM, Vucetich JA, Peterson RO, Lohmueller KE, Wayne1 RK.
776 2019. Genomic signatures of extensive inbreeding in Isle Royale wolves, a population on the
777 threshold of extinction. *Sci Adv* **5**.
778 Rosenthal WC, McIntyre PB, Lisi PJ, Prather Jr RB, Moody KN, Blum MJ, Hogan JD, Schoville
779 SD. 2021. Invasion and rapid adaptation of guppies (Poecilia reticulata) across the Hawaiian
780 Archipelago. *Evol Appl* **14**: 1747–1761.
781 Rougemont Q, Leroy T, Rondeau EB, Koop B, Bernatchez L. 2023. Allele surfing causes
782 maladaptation in a Pacific salmon of conservation concern. *PLoS Genet* **19**: e1010918.
783 Rougemont Q, Moore JS, Leroy T, Normandeau E, Rondeau EB, Withler RE, van Doornik DM,
784 Crane PA, Naish KA, Garza JC, et al. 2020. Demographic history shaped geographical patterns

785 of deleterious mutation load in a broadly distributed Pacific Salmon. *PLoS Genet* **16**.
786 Russell ST, Magurran AE. 2006. Intrinsic reproductive isolation between Trinidadian populations
787 of the guppy, Poecilia reticulata. *J Evol Biol* **19**: 1294–1303.
788 Schmidt C, Hoban S, Hunter M, Paz-Vinas I, Garroway CJ. 2023. Genetic diversity and IUCN Red
789 List status. *Conserv Biol* **37**: e14064.
790 Schories S, Meyer MK, Schartl M. 2009. Description of Poecilia (Acanthophacelus) obscura n.
791 sp.,(Teleostei: Poeciliidae), a new guppy species from western Trinidad, with remarks on P.
792 wingei and the status of the Endler s guppy. *Zootaxa* **2266**: 35–50.
793 Shaw PW, Carvalho GR, Seghers BH, Magurran AE. 1992. Genetic consequences of an artificial
794 introduction of guppies (Poecilia reticulata) in N Trinidad. *Proc - R Soc London, B*.
795 Sievers C, Willing E-M, Hoffmann M, Dreyer C, Ramnarine I, Magurran A. 2012. Reasons for the
796 invasive success of a guppy (Poecilia reticulata) population in Trinidad. *PLoS One* **7**: e38404.
797 Smeds L, Huson LSA, Ellegren H. 2024. Structural genomic variation in the inbred Scandinavian
798 wolf population contributes to the realized genetic load but is positively affected by
799 immigration. *Evol Appl* **17**: e13652.
800 Speak SA, Birley T, Bortoluzzi C, Clark MD, Percival-Alwyn L, Morales HE, Van Oosterhout C.
801 2023. Genomics-informed captive breeding can reduce inbreeding depression and the genetic
802 load in zoo populations. *Mol Ecol Resour* **24**: e13967.
803 Stewart GS, Morris MR, Genis AB, Szűcs M, Melbourne BA, Tavener SJ, Hufbauer RA. 2017. The
804 power of evolutionary rescue is constrained by genetic load. *Evol Appl* **10**: 731–741.
805 Stuart OP, Cleave R, Pearce K, Magrath MJL, Mikheyev AS. 2025. Purging of highly deleterious
806 mutations through an extreme bottleneck. *Mol Biol Evol* **42**: msaf079.
807 Tayeh A, Estoup A, Hufbauer RA, Ravigné V, Goryacheva I, Zakharov IA, Lombaert E, Facon B.
808 2013. Investigating the genetic load of an emblematic invasive species: the case of the invasive
809 harlequin ladybird Harmonia axyridis. *Ecol Evol* **3**: 864–871.
810 Teixeira JC, Huber CD. 2021. The inflated significance of neutral genetic diversity in conservation

genetics. *Proc Natl Acad Sci U S A* **118**: e2015096118.

van der Valk T, Díez-del-Molino D, Marques-Bonet T, Guschanski K, Dalén L. 2019. Historical Genomes Reveal the Genomic Consequences of Recent Population Decline in Eastern Gorillas. *Curr Biol* **29**: 165-170.e6.

van Oosterhout C, Speak SA, Birley T, Bortoluzzi C, Percival-Alwyn L, Urban LH, Groombridge JJ, Segelbacher G, Morales HE. 2026. Genomic erosion in the assessment of species extinction risk and recovery potential. *J Here* esag011.

Von Seth J, Dussex N, Díez-del-Molino D, Van Der Valk T, Kutschera VE, Kierczak M, Steiner CC, Liu S, Gilbert MTP, Sinding M-HS. 2021. Genomic insights into the conservation status of the world's last remaining Sumatran rhinoceros populations. *Nat Commun* **12**: 2393.

Wagner NK, Ochocki BM, Crawford KM, Compagnoni A, Miller TEX. 2017. Genetic mixture of multiple source populations accelerates invasive range expansion. *J Anim Ecol* **86**: 21–34.

Wallingford PD, Morelli TL, Allen JM, Beaury EM, Blumenthal DM, Bradley BA, Dukes JS, Early R, Fusco EJ, Goldberg DE. 2020. Adjusting the lens of invasion biology to focus on the impacts of climate-driven range shifts. *Nat Clim Chang* **10**: 398–405.

Whiting JR, Paris JR, van der Zee MJ, Parsons PJ, Weigel D, Fraser BA. 2021. Drainage-structuring of ancestral variation and a common functional pathway shape limited genomic convergence in natural high- And low-predation guppies. *PLoS Genet* **17**: 1–29.

Wilder AP, Supple MA, Subramanian A, Mudide A, Swofford R, Serres-Armero A, Steiner C, Koepfli K-P, Genereux DP, Karlsson EK. 2023. The contribution of historical processes to contemporary extinction risk in placental mammals. *Science (80-)* **380**: eabn5856.

Willi Y, Kristensen TN, Sgrò CM, Weeks AR, Ørsted M, Hoffmann AA. 2022. Conservation genetics as a management tool: The five best-supported paradigms to assist the management of threatened species. *Proc Natl Acad Sci* **119**: e2105076119.

Willing EM, Bentzen P, Van Oosterhout C, Hoffmann M, Cable J, Breden F, Weigel D, Dreyer C. 2010. Genome-wide single nucleotide polymorphisms reveal population history and adaptive

divergence in wild guppies. *Mol Ecol* **19**: 968–984.

Wooldridge B, Orland C, Enbody E, Escalona M, Mirchandani C, Corbett-Detig R, Kapp JD, Fletcher N, Cox-Ammann K, Raimondi P. 2024. Limited genomic signatures of population collapse in the critically endangered black abalone (Haliotis cracherodii). *Mol Ecol* e17362.

Wootton E, Robert C, Taillon J, Côté SD, Shafer ABA. 2023. Genomic health is dependent on long-term population demographic history. *Mol Ecol* **32**: 1943–1954.

Wright S. 1922. Coefficients of inbreeding and relationship. *Am Nat* **56**: 330–338.

Wright S. 1932. The roles of mutation, inbreeding, crossbreeding, and selection in evolution. In *Proc. of 6th Int. Congr. on Genetics, volume 1*, pp. 356–366, na.

Xie H-X, Liang X-X, Chen Z-Q, Li W-M, Mi C-R, Li M, Wu Z-J, Zhou X-M, Du W-G. 2022. Ancient demographics determine the effectiveness of genetic purging in endangered lizards. *Mol Biol Evol* **39**: msab359.

Xue Y, Prado-Martinez J, Sudmant PH, Narasimhan V, Ayub Q, Szpak M, Frandsen P, Chen Y, Yngvadottir B, Cooper DN. 2015. Mountain gorilla genomes reveal the impact of long-term population decline and inbreeding. *Science (80-)* **348**: 242–245.

Zayed A, Constantin ŞA, Packer L. 2007. Successful biological invasion despite a severe genetic load. *PLoS One* **2**: e868.

Zeitler L, Parisod C, Gilbert KJ. 2023. Purging due to self-fertilization does not prevent accumulation of expansion load. *PLoS Genet* **19**: e1010883.

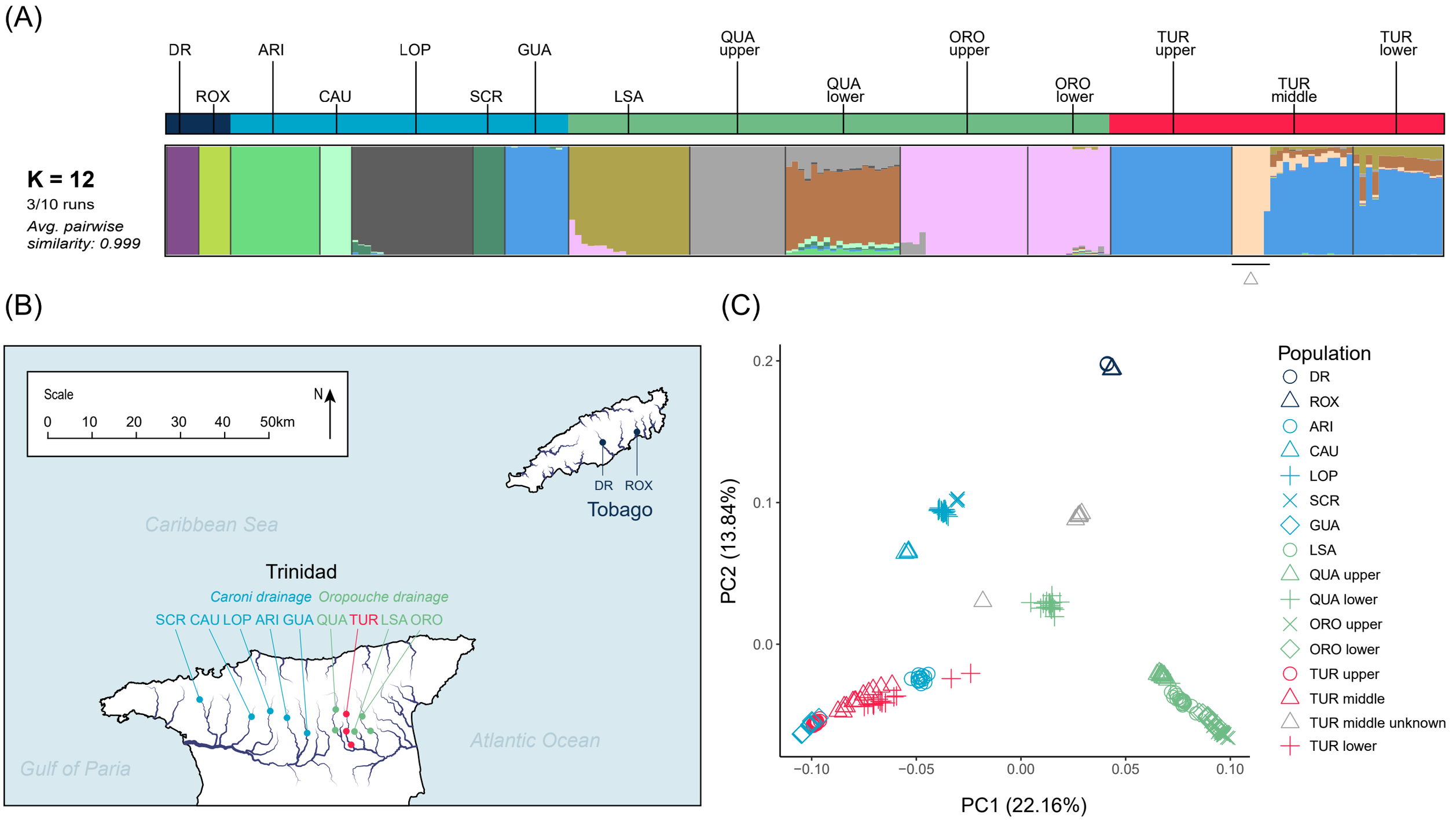
(A)
DR
ROX
ARI
CAU
LOP
SCR
GUA
LSA
QUA upper
QUA lower
ORO upper
ORO lower
TUR upper
TUR middle
TUR lower
K = 12
3/10 runs
Avg. pairwise similarity: 0.999
(B)
Scale
0 10 20 30 40 50km
N
DR ROX
Tobago
Caribbean Sea
Trinidad
Caroni drainage
Oropouche drainage
SCR CAU LOP ARI GUA QUA TUR LSA ORO
Atlantic Ocean
Gulf of Paria
(C)
PC2 (13.84%)
PC1 (22.16%)
0.2
0.1
0.0
−0.10
−0.05
0.00
0.05
0.10
Population
DR
ROX
ARI
CAU
LOP
SCR
GUA
LSA
QUA upper
QUA lower
ORO upper
ORO lower
TUR upper
TUR middle
TUR middle unknown
TUR lower

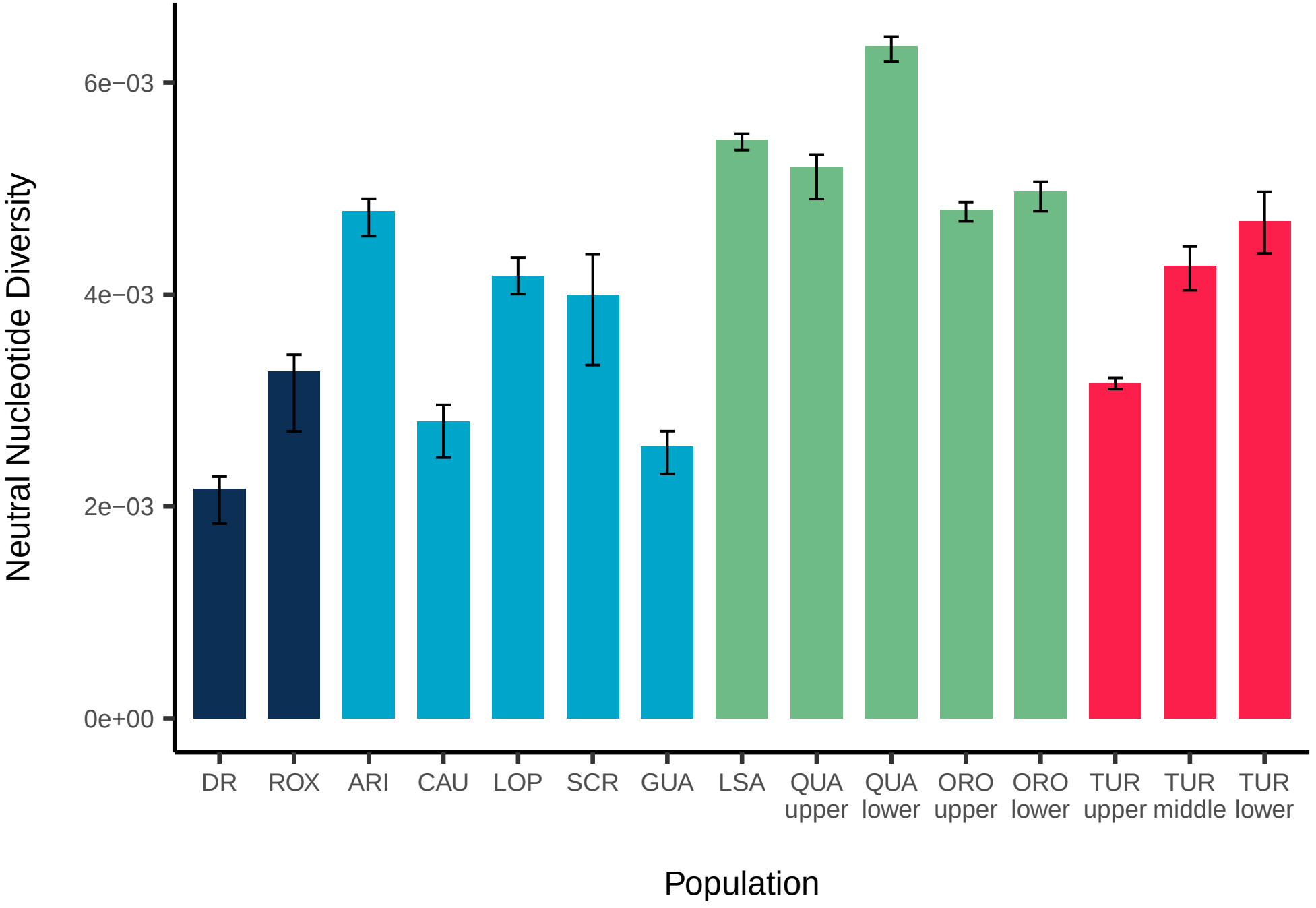
Neutral Nucleotide Diversity
6e−03
4e−03
2e−03
0e+00
DR
ROX
ARI
CAU
LOP
SCR
GUA
LSA
QUA upper
QUA lower
ORO upper
ORO lower
TUR upper
TUR middle
TUR lower
Population

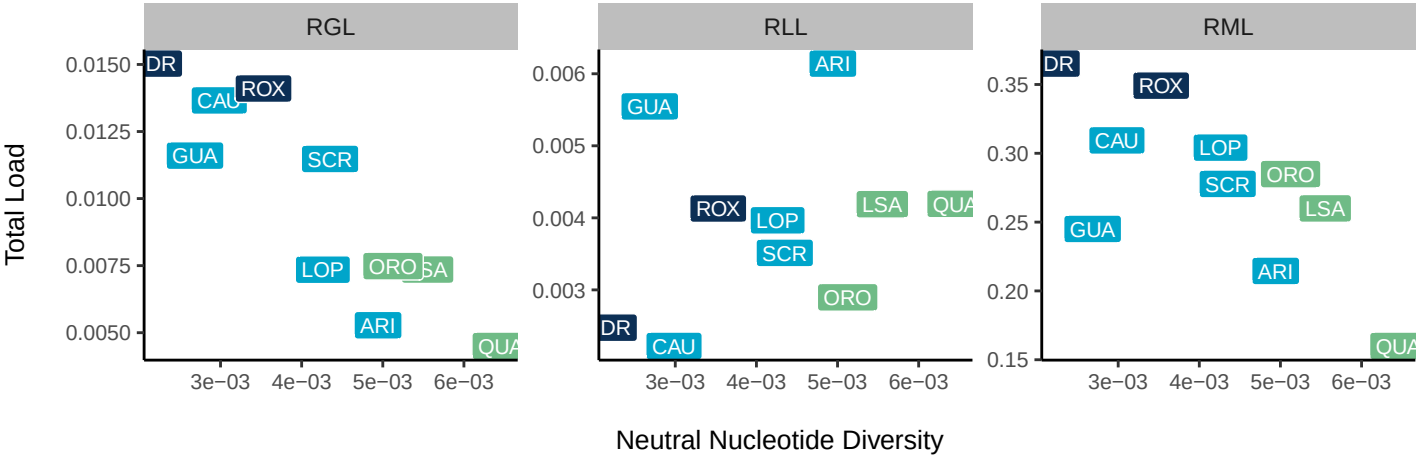
RGL
RLL
RML
Total Load
Neutral Nucleotide Diversity
0.0150
0.0125
0.0100
0.0075
0.0050
0.006
0.005
0.004
0.003
0.35
0.30
0.25
0.20
0.15
3e−03
4e−03
5e−03
6e−03
DR
ROX
CAU
GUA
SCR
LOP
ORO
LSA
ARI
QUA

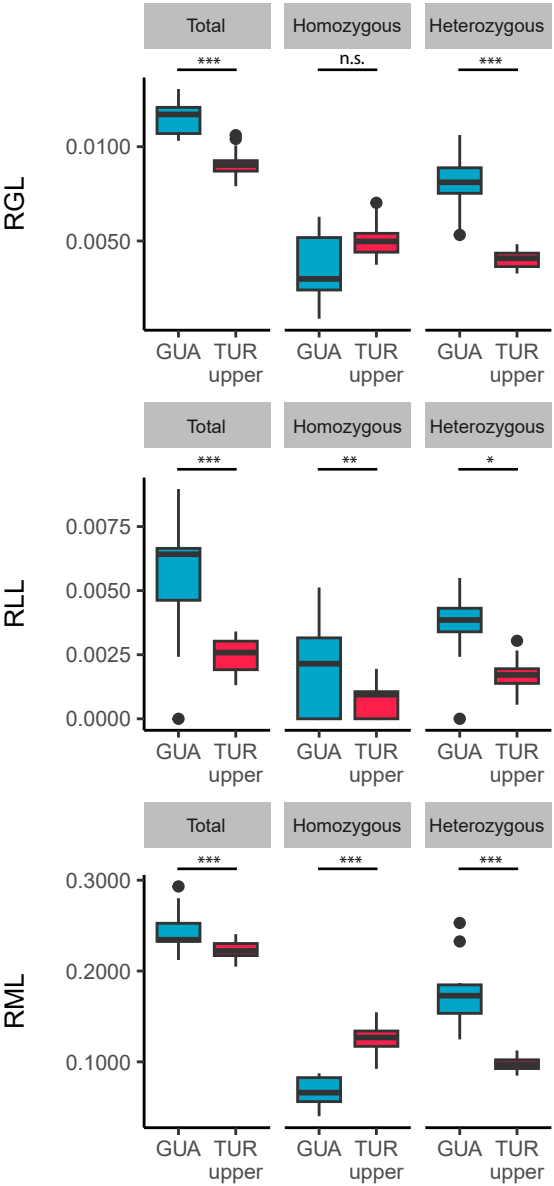
Total
Homozygous
Heterozygous
RGL
***
n.s.
***
0.0100
0.0050
GUA
TUR
upper
RLL
***
**
*
0.0075
0.0050
0.0025
0.0000
RML
***
***
***
0.3000
0.2000
0.1000

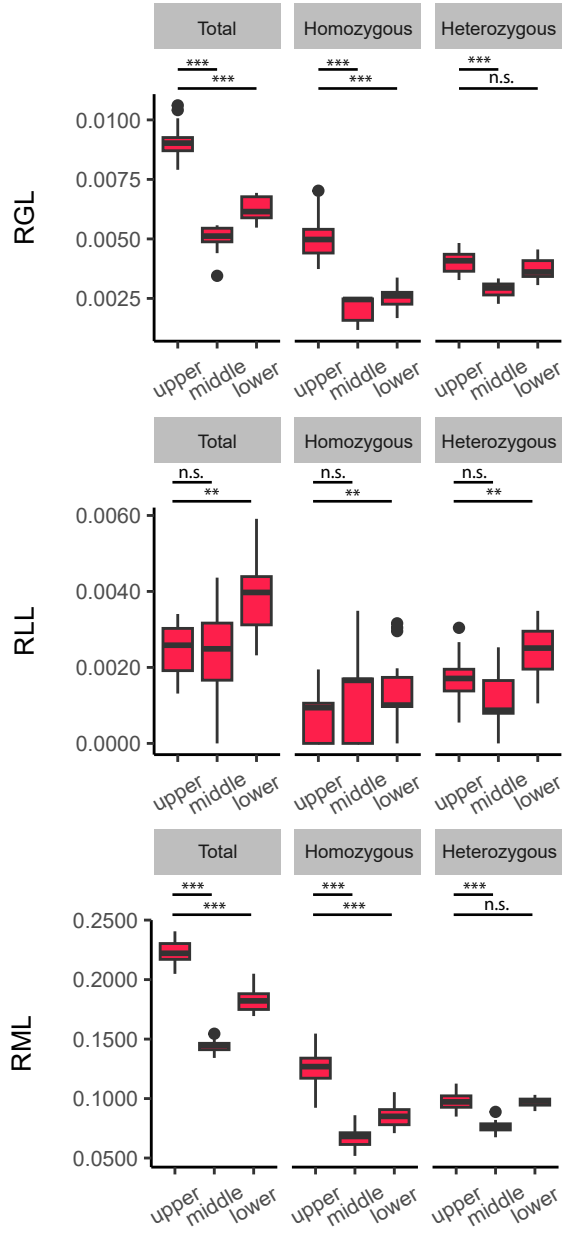
Total
Homozygous
Heterozygous
RGL
RLL
RML
***
**
n.s.
0.0100
0.0075
0.0050
0.0025
0.0060
0.0040
0.0020
0.0000
0.2500
0.2000
0.1500
0.1000
0.0500
upper
middle
lower